Optimization of Helium Extraction Processes Integrated with Nitrogen Removal Units: A Comparative Study

Homa Hamedi [a], Iftekhar A Karimi[a], cheiak@nus.edu.sg, Truls Gundersen[b], truls.gundersen@ntnu.no

a. Department of Chemical and Biomolecular Engineering, National University of Singapore (NUS). Address: 4 Engineering Drive 4, Singapore 117585.

b. Department of Energy and Process Engineering, Norwegian University of Science and Technology (NTNU). Address: Kolbjorn Hejes v. 1A, NO-7491, Trondheim, Norway.

Abstract

Helium is regarded as a vital gas to various industries such as medicine, aircraft manufacturing, electronics and fiber optics fabrication. Currently, natural gas reserves are considered the only viable resource for this rare element. When processing (helium-rich) natural gas, helium is generally recovered in the most downstream stage in conjunction with the nitrogen rejection unit (NRU). The feed to this unit is a nitrogen rich stream, and the product is either crude helium (50-70 mol% purity) or purified helium (99.99 mol% purity). Currently, the cryogenic distillation method is a common technology for a crude helium extraction unit (HeXU). The alternative method for this purpose is a membrane gas separation system, which is successfully used in other applications. This study aims to propose an energy-integrated scheme for each of the two helium separation technologies with a single-column NRU and to evaluate and compare them for different applications. Matlab programming has been used to model the membrane system and incorporate it into Aspen Hysys, which is used to simulate the rest of the process flowsheet. Next, the energy consumption of the systems was optimized using the particle swarm optimization method. An economic analysis was adopted to compare the two technologies for different applications in order to suggest a comprehensive map for HeXU technology selection.

Key words: helium extraction, nitrogen removal, gas permeation separation, cryogenic distillation, membrane separation, process integration

1 Introduction

1.1 Helium production

Helium is the second most abundant element in the universe after hydrogen. Due to its light weight, it easily escapes from the gravity and is exceedingly scarce in the Earth. The importance of this shortage can be realized upon consideration of its unique properties, such as low boiling point, low density, low solubility, high thermal conductivity and inertness, and its irreplaceable application in both scientific research and industry. For instance, this inert gas is critical to technologies such as MRI scanners, aerospace and aircraft manufacturing, industrial-leak detection systems, electronics and fiber optics fabrication, welding and nuclear research facilities.

Although the Earth's atmosphere is the main terrestrial inventory of helium, it has been widely concluded that extraction of helium from the air as a primary product is inviable due to its very low concentration of 5 ppm. At present, the only economical helium source is proven to be natural gas (NG) reserves, where it has a concentration between 0.3 and 2 mol% in so-called helium-rich NG fields and as high as 8 mol% only in certain fields. The USA has so far been the world's leading helium supplier with approximately 55%

share of global supply in 2016, followed by Qatar (33%), Algeria (6%), Australia (3%), Russia (2%) and Poland (1%). Also, Tanzania is expected to have a considerable contribution in the future after the discovery of a natural store of helium found in the Rift valley in 2015 (Burite, 2016).

Helium is marketed in two specifications: crude helium, which typically contains 50-70 mol% helium, and purified helium with >99.99 mol% purity. The extraction of crude helium or upgraded helium (90 mol%) from natural gas typically requires four processing steps. The first step is to remove the typical impurities in the gas, namely carbon dioxide, hydrogen sulfide, water, and mercury. The second step involves the extraction of heavier hydrocarbons. The third step is called the nitrogen rejection unit (NRU), which separates most of the remaining methane gas from the mixture of nitrogen and helium. The final step is the helium extraction unit (HeXU), which can be either a cryogenic distillation-based HeXU process (CDBHeXU) or a membrane-based HeXU (MBHeXU). It recovers helium from the nitrogen-rich stream and produces either the crude helium (50-70 mol%) for sales or the upgraded helium with 90 mol% purity for further purification. In the latter case, the 90 mol% pure helium is then purified to 99.99 mol% using pressure swing adsorption (PSA). It is obvious that when nitrogen is utilized for enhanced oil/gas recovery (EOR/EGR), 90 mol% purity is favorable due to the higher amount of nitrogen recovery.

Figure 1 depicts the block flow diagram of helium production for both pipeline natural gas (PNG), type A, and liquefied natural gas (LNG), type B, which is only suitable when the feed nitrogen is less than 5-8 mol% or the plant's fuel gas consumption is high. The type A is also applicable for LNG plants with high nitrogen content. In this case, the sales gas product (Figure 1a) is routed to LNG plants for further processing, which is not shown in the figure. The scope of the current study is limited to the HeXU and NRU in Figure 1a as shown by dashed lines in this figure. As illustrated in the scheme, the extracted helium in the HeXU can either be marketed at 50-70 mol% purity (crude helium) or purified further to 90 mol% and then transferred to PSA and liquefaction units to produce purified helium. In type A configuration, the NRU process is a stand-alone process and the feed into the HeXU contains only helium and nitrogen at high pressure. Thus, the NRU hereafter in this study indicates the type A process otherwise specified.

Furthermore, it should be noted that most of the NG reserves with high helium contents typically have a significant amount of nitrogen. This is why HeXU and NRU facilities are required simultaneously and usually integrated to have a higher energy efficiency. Moreover, it should be noted that the PSA technology is not worth considered for the HeXU section due to a low energy efficiency. This is because it adsorbs nitrogen at high pressures and desorbs it at atmospheric pressure with no use of its pressure exergy. However, it is typically utilized at the final stage (helium purification) where the concentration of nitrogen is significantly reduced in order to approach the desired purity of 99.99% and remove any other impurities.

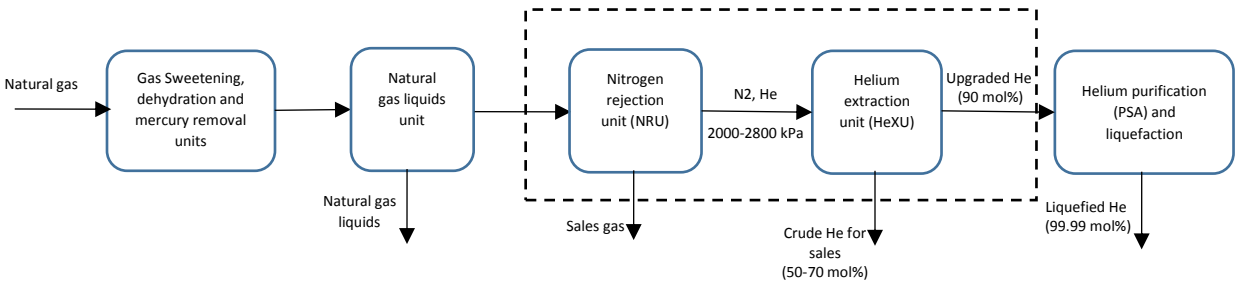

Figure 1a. Natural gas processing steps type A for NG plants and LNG with high nitrogen content

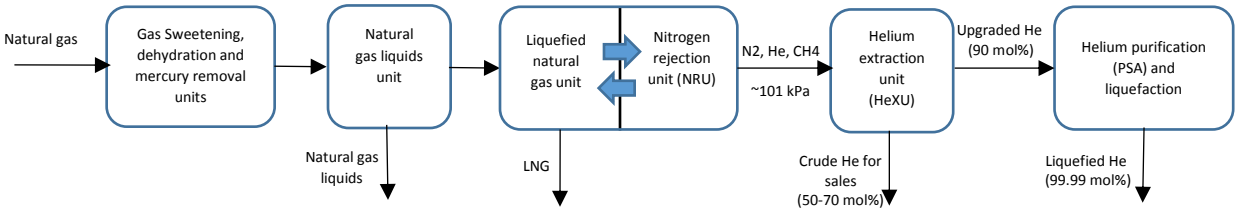

Figure 1b. Natural gas processing steps type B for LNG plants with low nitrogen content

1.2 Nitrogen rejection unit

There are two different cryogenic NRU configurations: single-column design and multi-column design. The former is more suitable to accommodate the HeXU as an integral part due to the simultaneous provision of high pressure and low temperature for the helium-rich stream (Hamedi et al., 2018). A typical single-column design is presented in Figure 2. As shown in the process scheme, the single-column design is enhanced by a heat-pump cycle, with methane as a refrigerant, between the condenser and reboiler to partly provide the process refrigeration requirement. The column feed is cooled by the sales gas product and nitrogen effluent in the entrance heat exchanger and then throttled in the inlet valve. The two heat exchangers are not integrated in the conventional single column design. This potential integration is able to reduce the power consumption significantly, especially when the feed nitrogen or helium content is not too high. In fact, in this integrated design, we are able to take advantage of the self-heating reboiler (SHR) system in which the reboiler heat requirement is provided by the inlet feed instead of the refrigeration cycle in the conventional scheme. In this design, the refrigerant is cooled by the sales gas stream and heated by the reflux. This arrangement decreases the work consumption of the heat pump cycle. This is because the new heating and cooling media, which are the sales gas and condenser respectively, have a lower temperature difference as compared to the temperature difference between reboiler and condenser in the conventional design. Nevertheless, the SHR system cannot be utilized when the nitrogen or helium content of the feed exceeds beyond some specific values due to the limitation of the lowest cooling temperature which can be provided by methane as the refrigerant at atmospheric pressure. Because of this constraint, the column operating pressure cannot be reduced to accommodate the opportunity for the SHR arrangement. A more detailed discussion of this will be provided in Section 2.

1.3 Objective and Motivation

All the commercial process configurations of type B, with the CDBHeXU, are comprehensively reviewed and compared by Kim & Gundersen (2015). The MBHeXU for this type of process is also investigated and evaluated economically (Scholes & Ghosh, 2016; Scholes et al., 2017). The study also investigates the effect of membrane selectivity in single, double and three stage membrane processes. It is concluded that single-stage membrane systems cannot be a practical choice to produce crude helium because of the low pressure of the NRU exit stream, which requires significant compression work.

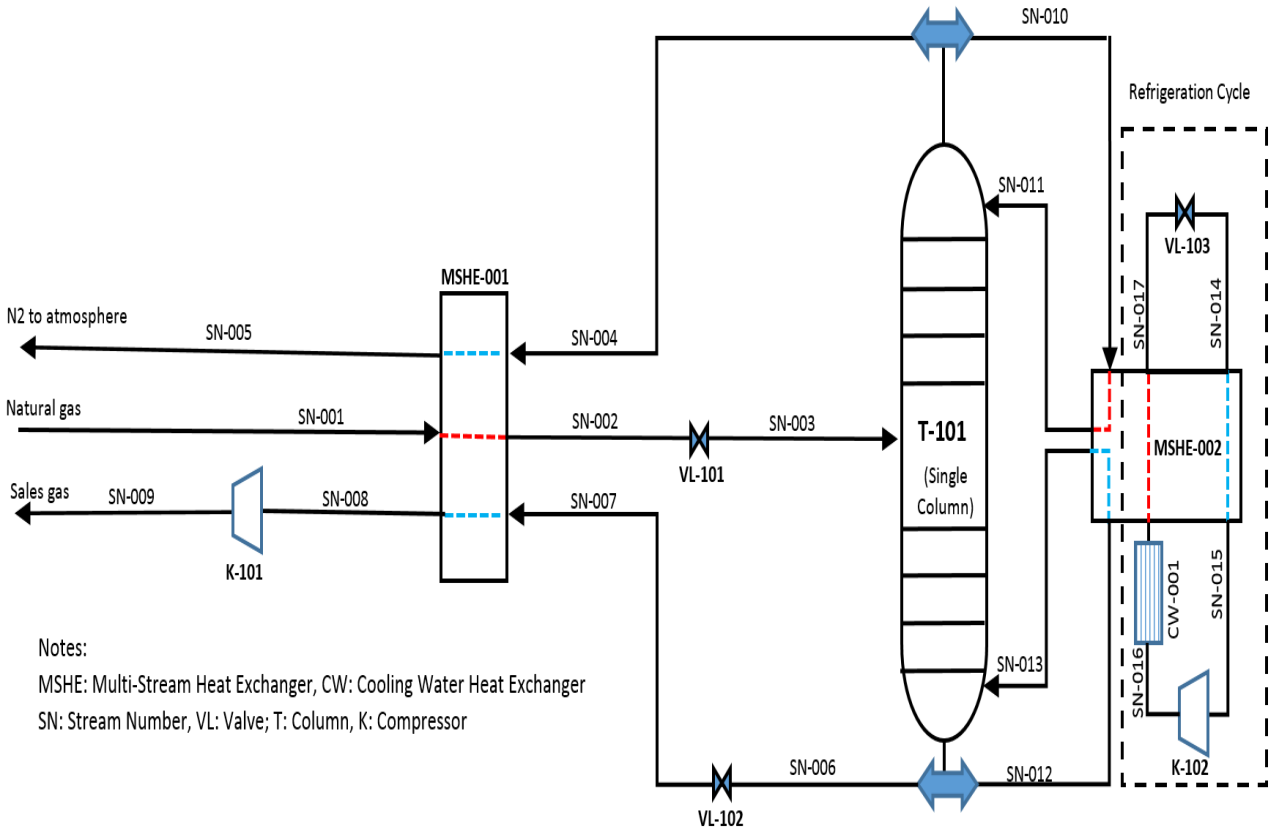

Figure 2. A typical single-column design for the nitrogen rejection unit

In contrast, several articles compare the performance of NRU type A processes (Hamedi et al., 2018; MacKenzie et al., 2002; Rufford et al., 2012). However, little literature has studied the integrated NRU and cryogenic distillation-based HeXU processes as Type A, which is illustrated in Figure 1a. To the best of our knowledge, there is only one investigation on this process category, which compares both CDBHeXU and MBHeXU embedded into a single-column NRU (Alders et al., 2017). However, they used a hypothetical simulation for the NRU section to derive feed conditions for the HeXU. Thus, the simulation may not represent a real integrated NRU and HeXU process and the treatment cost may not be reliable in real situations. This indicates a need to investigate the integrated NRU and HeXU process in a more accurate and practical way to present an actual economic evaluation and a fair comparison between the two alternatives for the HeXU.

This study seeks to propose two different heat-integrated HeXU designs, namely the CDBHeXU and MBHeXU, which are incorporated into the single-column NRU. Next, we optimize the entire system in terms of power consumption, evaluate and compare them in different scenarios. In summary, this investigation suggests a comprehensive map for technology selection of the HeXU for the type A process as illustrated in Figure 1a.

2 Process description and simulation

2.1 Single-column NRU with CDBHeXU

Figure 3a-c illustrate the process flow diagram (PFD) of an integrated NRU and CDBHeXU process, which is represented with CDBHeXU-NRU hereafter, for three different cases respectively:

a. Crude helium (50-70 mol%) production and nitrogen released into the atmosphere
b. Upgraded helium (90 mol%) production and nitrogen released into the atmosphere
c. Upgraded helium (90 mol%) production and nitrogen compressed to higher pressure for EOR/EGR applications

It should be noted that when the upgraded helium (cases B and C) is a product, T-201 needs both stripping and rectification sections, while crude helium production only needs a stripping section. It is obvious that the EOR/EGR scenario is not considered for the crude helium production (case A) due to the low nitrogen recovery. In cases B and C, the upgraded helium should be compressed to a higher pressure (~3000 kPa) for the downstream PSA treatment.

As shown in Figure 3a-c, the NRU section, which is common in all the schemes, uses a cryogenic distillation column aided by a methane refrigeration cycle to mainly cater the reflux cooling requirement. Two Joule-Thomson expansion valves (VL- 101 located on the column feed (SN-102) and VL-102 on the sales gas product (SN-108)) are also devised to pre-cool the column feed. To maximize cold energy recovery, we merge the two MSHEs in the conventional design (Figure 2) into a multi-stream heat exchanger (MSHE-101). This heat integration takes advantage of the SHR arrangement. The feed gas (SN-101) is partly pre-cooled by the boil-up stream (SN-106), which is only used to cool the refrigerant in a conventional process design. This modification significantly decreases the power consumption for feeds with lower nitrogen and helium contents. In this case, the boil-up heating can be fully provided by the column feed (SN-101) and the refrigeration cycle needs to pump heat between the reflux stream (SN-104) and the sales gas (SN-109).

The overhead stream of T-101, which has a higher helium content, is routed to the HeXU, where it is separated to nitrogen and crude helium using a cryogenic distillation column (T-201). The nitrogen product of T-201 is split into two streams using Tee-201 with one throttled in VL-202 and another pumped to a higher pressure. They provide two different temperatures to cool the feed (SN-201) and supply the condenser cooling requirement for Cases B and C.

In Cases A and B, the high-pressure nitrogen (SN-118) is expanded in E-101, covering some portion of the compressor work consumption. Then it joins the low-pressure nitrogen (SN-119) and is released into the atmosphere. In Case C, the low-pressure nitrogen (SN-119) is compressed in K-103 and merges with the high-pressure nitrogen (SN-122) to be further compressed to the desired product pressure.

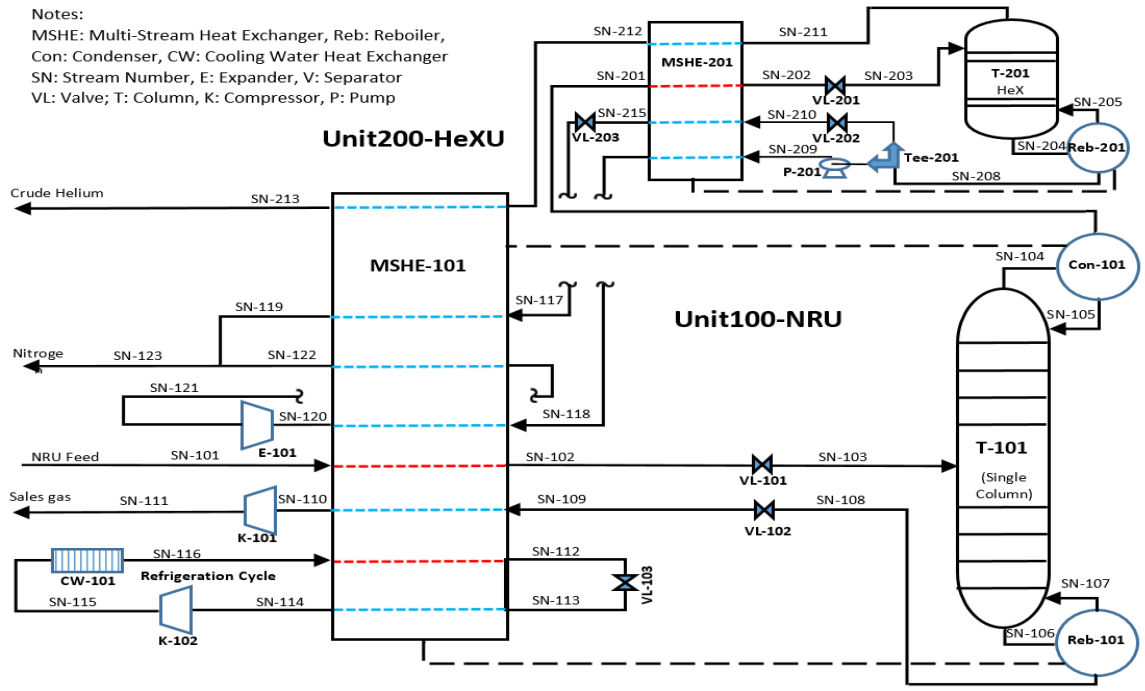

Figure 3a. Integrated CDHeXU-NRU for crude helium production and N2 release into the atmosphere (Case A)

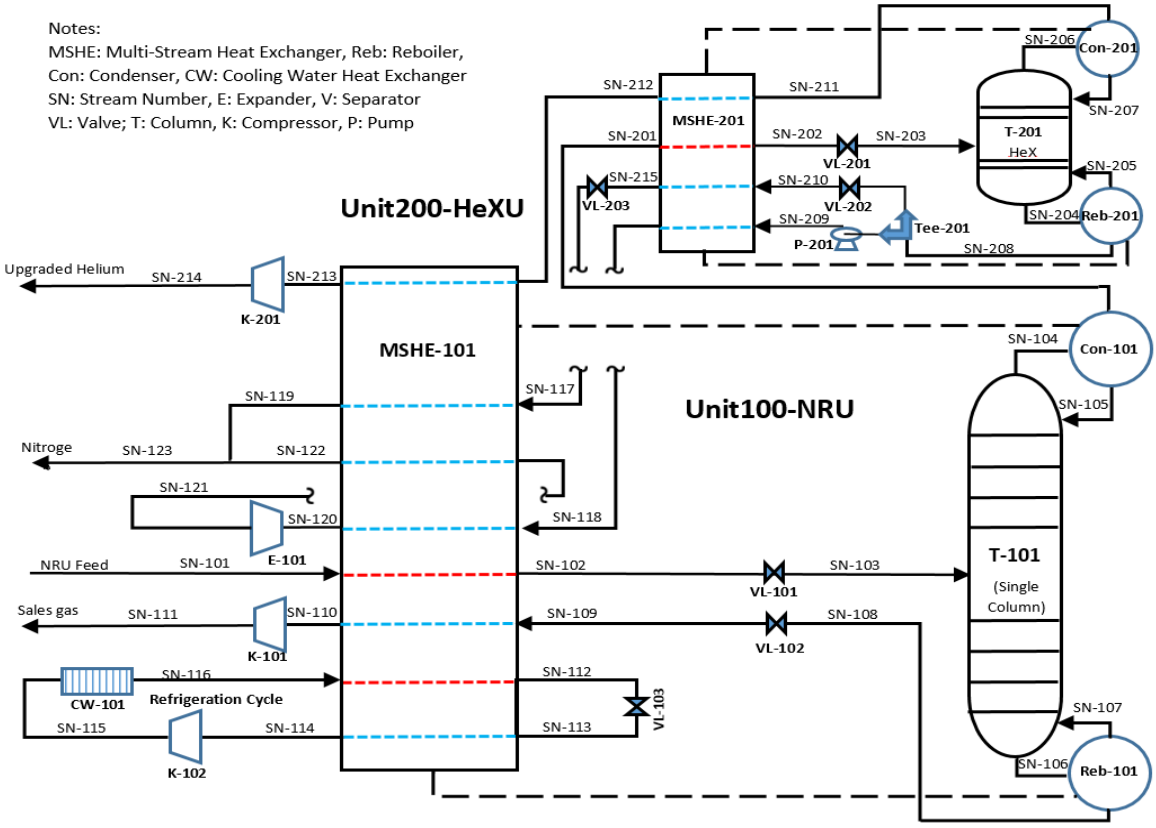

Figure 3b. Integrated CDHeXU-NRU for upgraded helium production and N2 release into the atmosphere (Case B)

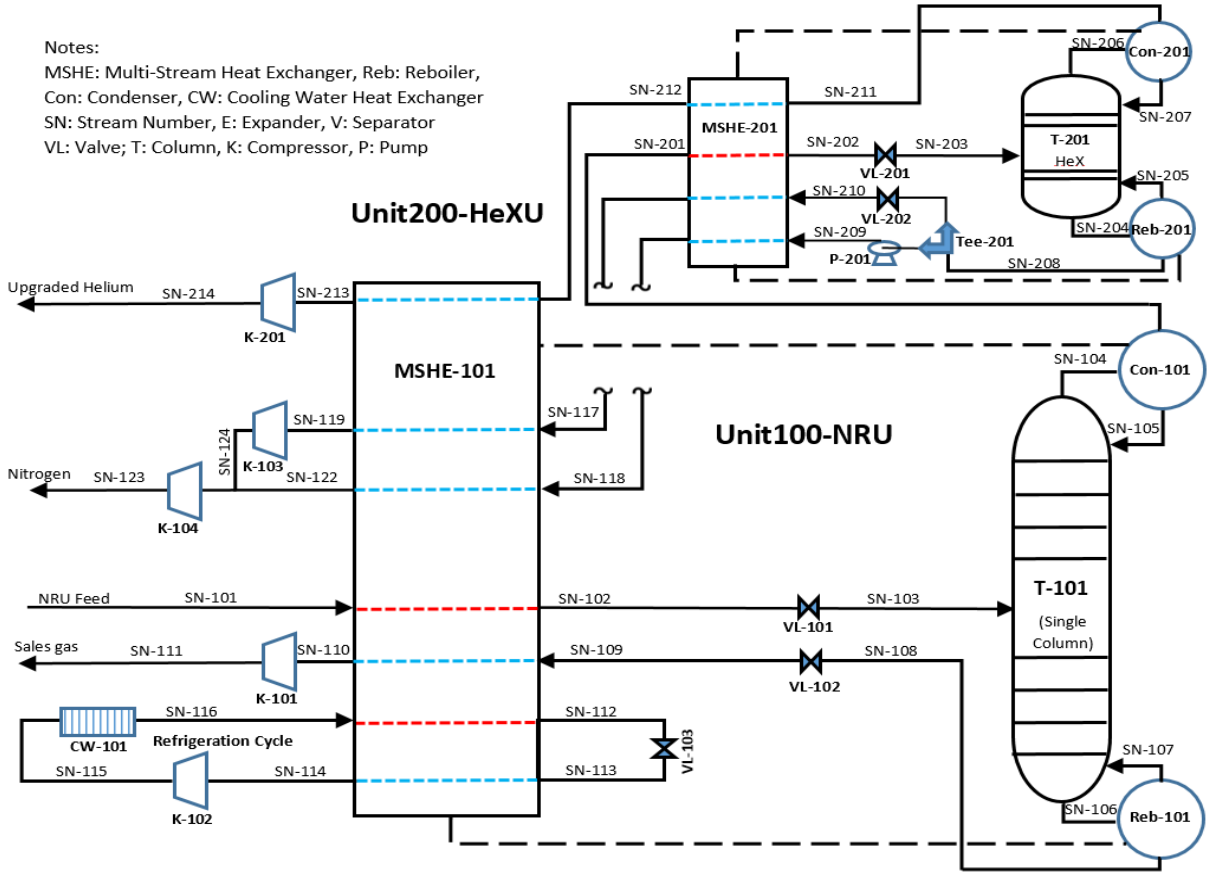

Figure 3c. Integrated CDHeXU-NRU for upgraded helium production and pressurized N2 for EOR/EGR (Case C)

The helium (SN-213) is produced from the column top. Then, it is compressed in K-201 for Cases B and C to be ready for the downstream PSA separation.

The process simulations were done in Aspen Hysys (V9) using the Peng-Robinson fluid package. HYSIM inside-out method was chosen for column simulation.

K-101, K-102 and K-103 are multi-stage centrifugal compressors with interstage cooling using water. Due to a lower pressure ratio, K-101 has two stages, whereas K-102 and K-103 use three-stage compression. K-104 is a one-stage centrifugal compressor. An oil-injected screw-type compressor was used for K-201as common in industry for helium compression due to its high heat capacity ratio.

2.2 Single-column NRU with MBHeXU

Figure 4 shows a schematic diagram of an integrated NRU and MBHeXU process, which is referred to as MBHeXU-NRU hereafter. We assume the same three scenarios mentioned in Section 2.1. The diagram can represent all the three scenarios: Case A when K-201 and K-203 are removed, Case B if K-201 is removed, and Case C if E-101 is removed. It should be noted that when the nitrogen product has a high pressure, such as Case C, K-201 should be placed prior to Mem-201 since this configuration also helps the permeation process. However, using K-201 in Cases A and B, in which nitrogen is released into the atmosphere, in order just to help the permeate separation, is not economical.

The main difference between this design and the previous ones is the HeXU, where we utilize a two-stage membrane system instead of a cryogenic distillation column. As can be seen in Figure 4, the MBHeXU cannot be located directly downstream of the NRU column due to the operating temperature requirement of membranes. In fact, the NRU column's overhead stream has a cryogenic temperature which is not applicable for membrane systems. Thus, the feed stream (SN-119) should be heated prior to entering the MBHeXU. Furthermore, there is a recycle stream (SN-208) between the two membranes (Mem-201 and Mem-202) which significantly enhances helium recovery. The crude or upgraded helium (SN-209) is drawn from the second membrane, Mem-202 and compressed in Cases B and C. The nitrogen (SN-205) from the first stage membrane is either released into the atmosphere after one-stage expansion and thereby losing its cooling energy (Cases A and B) or delivered with a higher pressure for further applications (Case C).

K-101, K-102 and K-202 are multi-stage centrifugal compressors with interstage cooling using water. Due to a lower pressure ratio, K-101 has two stages, whereas K-102 and K-202 use three-stage compression. K-201 is a one-stage centrifugal compressor. An oil-injected screw compressor was used for K-203.

A diffusion-based model of cross-flow gas permeation, based on a study by Coker et al., 1998, was programmed in Matlab and incorporated into Aspen Hysys to undertake the desired separation. The cross-flow pattern is widely used for commercial membrane modules and is the most practical model for gas permeation processes. Also, vacuum condition is avoided on the permeate side as it requires larger and more complicated equipment, as well as larger membrane area (Baker & Wiley, 2012; Gottschlich et al., 1989; Merkel et al., 2010). Therefore, the permeate pressure can never be less than atmospheric.

The cascade configuration, in which the retentate of the second membrane is recycled to the first membrane feed, was selected in this study. This configuration is proven to be the best when the feed and product compositions are very different, such as the separation under investigation (Gottschlich et al., 1989).

For specified membrane properties and permeation pressures, as well as given total recovery, the following relationship exists between the two membrane recoveries.

$$Recovery_{Mem-202} = \frac{1-{}^{1}/_{Recovery_{Mem-201}}}{1-1/Recovery_{total}} \quad \text{where} \quad Recovery_{Mem-201} \geq Recovery_{total} \qquad \text{Eq. (1)}$$

where $Recovery_{total}$, $Recovery_{Mem-201}$ and $Recovery_{Mem-202}$ represent the total, the first stage membrane, and the second stage membrane helium recovery respectively (Figure 4). Accordingly, $Recovery_{Mem-201}$ is the only variable which should be set to achieve the desired purity for the crude helium product. Also, $Recovery_{Mem-202}$ is only valid when $Recovery_{Mem-201}$ is larger than the total recovery; otherwise the former will be higher than unity (which is not possible). It should be noted that when $Recovery_{Mem-201}$ and the total recovery are equal (or in other words, $Recovery_{Mem-202}$ is unity), the recycle flow (or the second stage retentate) becomes zero, which is equivalent to one-stage membrane arrangement. Eq. 1 is proven in Appendix A.

It is worth highlighting that product recovery and purity specifications may not be met in a one-stage membrane regardless of how large the membrane is. As a matter of fact, there is an inverse relationship between purity and recovery. In other words, if the membrane is incremented along its length, the most helium-rich permeate flow is produced near the membrane inlet where helium concentration is the highest. When moving forward, the purity of the permeate flow decreases since the helium concentration on the feed side declines along the membrane. Thus, as membrane length (or membrane area) increases, the final

product purity decreases while the recovery increases. Accordingly, for given feed and permeate pressures and recovery rate, it is possible to check whether one-stage membrane can meet the purity specification or not.

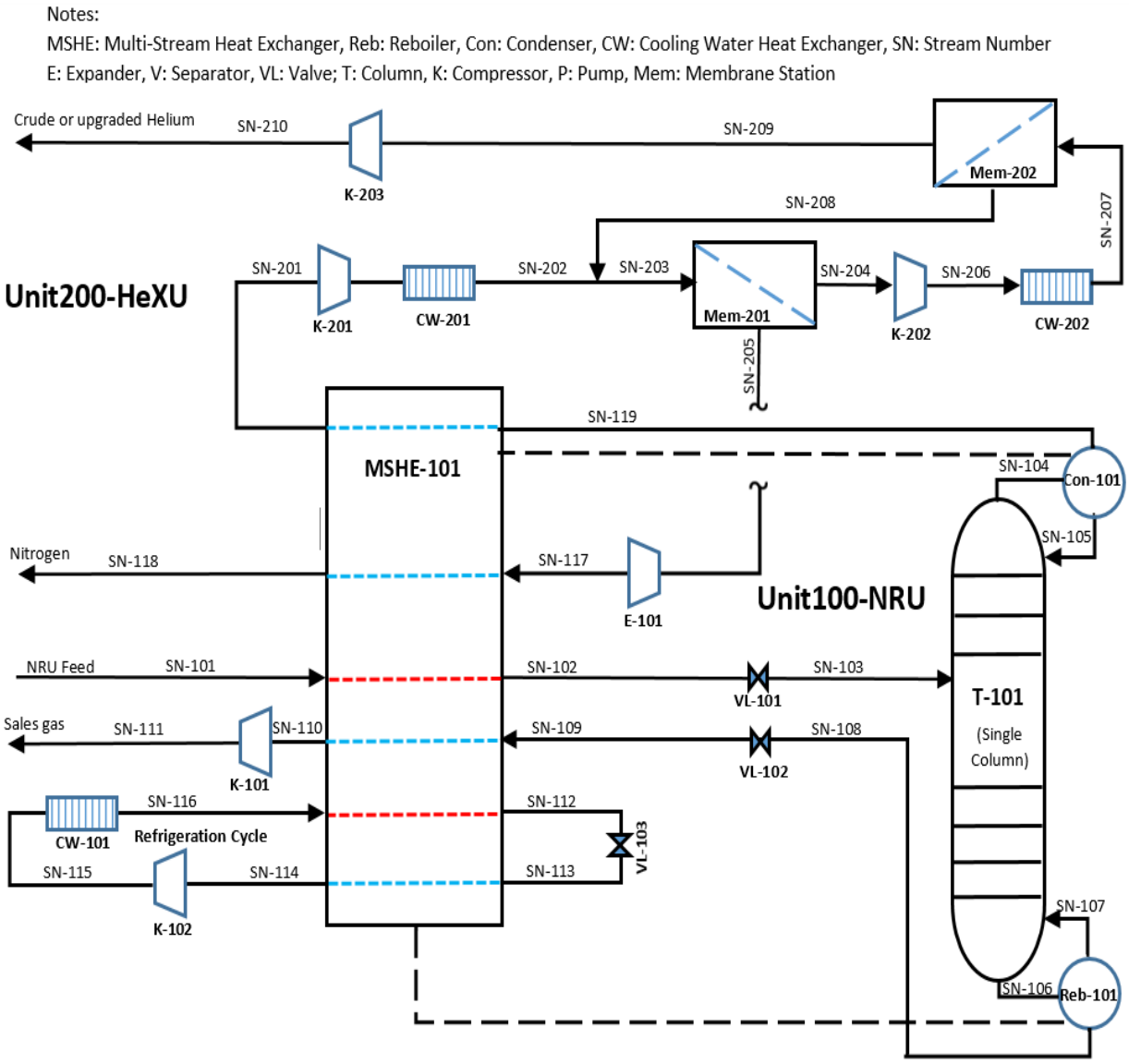

Figure 4. Integrated MBHeXU-NRU for Cases A, B and C

3 Parametric optimization

To compare the two processes in a fair way, the key parameters for each process in Figures 3 and 4 were identified and the net power consumption was minimized using Particle Swarm Optimization (PSO). PSO is a population-based stochastic optimization technique developed by Kennedy and Eberhart, 1995. Over the past years, PSO has been successfully applied to many chemical engineering problems (Cao et al., 2017; Clarke et al., 2014; Sadeghzadeh et al., 2015; Siddhartha et al., 2012). It is shown that this method

outperforms other meta-heuristic methods as it is computationally faster with better optimal solutions (Eghbal et al., 2011; Elbeltagi et al., 2005; Hassan et al., 2005; Panduro et al., 2009). This technique is classified as a non-derivative approach since it explores the search space without any information about problem structures or gradients. Therefore, it can tackle problems with objective functions evaluated by black-box software like the problem under investigation. A detailed description of the methods is available in Kennedy and Eberhart, 1995.

Table 1 presents the decision variables for each design case. The objective function of each process is the sum of the power consumption corresponding to pumps and compressors minus the expander power generation, subject to the minimum temperature approach for any MSHE involved in the processes. In other words, the temperature approach of each MSHE should be greater than or equal to the corresponding minimum temperature approach specified in Table 2. In addition to the MSHE-related constraints, a large penalty value is also applied for any module, including sets and adjustments, which does not converge. However, for MSHEs, the penalty values are proportional to the magnitude of temperature cross. Purity and recovery are imposed as "specs" on the distillation column sub-flowsheets in Aspen HYSYS. The conditions of the reflux and boil-up streams from inside the distillation column sub-flowsheet were copied to create the streams entering MSHE-101. Furthermore, Eq. 1 gives us a relation between two recoveries for a known total recovery. Thus, one recovery is adjusted to meet the helium product purity. This trick eliminated the purity constraint for the two-stage membrane system.

The particle size for each variable in the PSO was considered to be 20. The maximum iteration and trial numbers used were 200 and 10 respectively. Both individual and global acceleration factors were assumed to be 1.0. The minimum and maximum inertia weights were considered to be 0.5 and 1 respectively.

Table 1. Decision variables (Press:Pressure, Tem:Temperature, VF:Vapor Fraction, SR:Split Ratio, F:Flowrate)

Process type	Distillation-based HeXU (CDBHeXU)			Membrane-based HeXU (MBHeXU)		
Case	Case A	Case B	Case C	Case A	Case B	Case C
Number of the decision variables	14	17	16	11	12	11
x1	SN-103-Press	SN-103-Press	SN-103-Press	SN-103-Press	SN-103-Press	SN-103-Press
x2	SN-103-VF	SN-103-VF	SN-103-VF	SN-103-VF	SN-103-VF	SN-103-VF
x3	SN-109-Press	SN-109-Press	SN-109-Press	SN-109-Press	SN-109-Press	SN-109-Press
x4	SN-110-Tem	SN-110-Tem	SN-110-Tem	SN-110-Tem	SN-110-Tem	SN-110-Tem
x5	SN-119-Tem	SN-119-Tem	SN-119-Tem	SN-118-Tem	SN-118-Tem	SN-201-Tem
x6	SN-120-Tem	SN-120-Tem	SN-122-Tem	SN-201-Tem	SN-201-Tem	SN-116-F
x7	SN-122-Tem	SN-122-Tem	SN-213-Tem	SN-116-F	SN-116-F	SN-116-Press
x8	SN-213-Tem	SN-213-Tem	SN-202-Tem	SN-116-Press	SN-116-Press	SN-112-Tem
x9	Tee-201-SR	SN-202-Tem	SN-203-Press	SN-112-Tem	SN-112-Tem	SN-113-Press
x10	SN-209-Press	SN-203-Press	Tee-201-SR	SN-113-Press	SN-113-Press	SN-204-Press
x11	SN-116-F	Tee-201-SR	SN-209-Press	SN-204-Press	SN-204-Press	SN-209-Press
x12	SN-116-Press	SN-209-Press	SN-210-Press	----	SN-209-Press	----
x13	SN-112-Tem	SN-210-Press	SN-116-F	----	----	----
x14	SN-113-Press	SN-116-F	SN-116-Press	----	----	----
x15	----	SN-116-Press	SN-112-Tem	----	----	----
x16	----	SN-112-Tem	SN-113-Press	----	----	----
x17	----	SN-113-Press	----	----	----	----

For the Distillation-based HeXU, each optimization run took 6 to 8 hours. For the membrane-based HeXU, each run took more time, about 12 hours. The latter is higher, because the membrane model was written in MATLAB and Hysys-Matlab interface slows down computations considerably. All computations were done on an Intel®Core (TM) i5-6600 workstation with 3.3 GHz CPU and 16GB RAM.

4 Design Data and Specifications

Table 2 shows the specifications and design data used in this study. Two different nitrogen contents, 15 and 30 mol%, are considered in the inlet feed gas (SN-101 in Figure 3 and 4) containing various helium mole fractions of 0.3, 0.5, 1 and 2 mol%. The feed conditions are adopted from MacKenzie et al. (2002).

Table 2. Design data and specifications

Design specification	Value
Feed flowrate, kmole/s	0.54
Feed pressure, kPa	3104
Feed temperature, °C	298.15
Compressor adiabatic efficiency	0.75
Expander adiabatic efficiency	0.85
Motor efficiency	0.83
Min temperature approach in MSHEs in NRU, °C	2
Min temperature approach in MSHEs in HeXU, °C	1
Pressure Drop for MSHE, kPa	20
Methane fraction in NRU column's overhead, mol%	1
Nitrogen fraction in NRU column's bottom, mol%	3
Helium recovery rate for Case A, mol%	99
Helium recovery rate for Cases B and C, mol%	90
Crude helium purity, mol%	70
Upgraded helium purity, mol%	90
Minimum nitrogen effluent pressure, kPa	110
Helium product pressure for Case A, kPa	600
Minimum nitrogen effluent pressure for Cases B and C, kPa	3000
NG sales gas pressure, kPa	1827
Number of stages for nitrogen removal column	20
Pressure drop for nitrogen removal column, kPa	20
Number of stages for helium recovery column	5
Pressure drop for helium recovery column, kPa	5
Tray efficiency, percentage	80
Membrane selectivity	155 and 811
Membrane helium permeability (Barrer)	62 and 22.5
Membrane thickness (μm)	20
Cooling water temperature, °C	293.15
Min temperature approach for cooling water heat exchanger, °C	5

5 Results

5.1 Case A: crude helium and atmospheric nitrogen

The differences in performance of the MB-HeXU-NRU with two different selectivities (155 and 811) and the CDBHeXU-NRU are shown in Figures 5 and 6 for 15 mol% and 30 mol% nitrogen contents

respectively. 155 and 811 selectivities correspond to benzoxazole-co-pyrrolone and polypyrrolone-6FDA/PMDA (10/90) respectively and are obtained from Soleimany et al., 2017. 811 is the highest He/N2 selectivity reported in the literature (Soleimany et al., 2017), but due to its low permeability, this choice is not viable as the required permeation area is 10-13 times larger than that of 155 selectivity. In fact, the only reason for considering this high selectivity is to show the impact and significance of this parameter on the system performance.

As can be seen in the figures, the CDBHeXU-NRU shows a better performance in terms of power consumption for both 15 and 30 mol% nitrogen. As it is expected, the MBHeXU-NRU with a higher selectivity (811) needs less power to carry out the separation. However, it still fails to outperform the CDBHeXU-NRU.

It should be noted that there are two reasons why the performance differences of the MBHeXU-NRU and the CDBHeXU-NRU are higher for 30 mol% nitrogen compared with 15 mol%. First, for the same helium content in the main feed, the feed flowrate into the HeXU is higher in the case with 30 mol%. Thus, the HeXU needs proportionally higher energy to carry out the separation. Secondly, for the same helium content in the main feed, helium concentration in the HeXU feed is lower for 30 mol% nitrogen. As shown in Figure 7, when helium decreases in the HeXU feed, the power requirement for membrane separation increases. Therefore, the higher flowrate and lower helium concentration in the HeXU feed lead to a higher power consumption difference for 30 mol% nitrogen.

Furthermore, Figure 7 suggests why the MBHeXU-NRU in Figure 6 has a curved shape with a minimum. It can be observed, as helium increases in the feed, the NRU power consumption increases. However, as helium decreases, the membrane power consumption increases. These two opposite trends cause a minimum in Figure 6.

Moreover, there is a kink for the CDBHeXU-NRU plot in Figure 5. This is because, for 15 mol% nitrogen and 0.3 to 1 mol% helium in the main feed, the NRU uses the SHR arrangement. As mentioned earlier, SHR can reduce the power consumption significantly when the nitrogen and helium concentration is not too high. For 15 mol% nitrogen and 2 mol% helium, the SHR arrangement cannot be utilized due to the NRU column's reflux temperature. Also, 30 mol% nitrogen with any helium concentration cannot use the SHR.

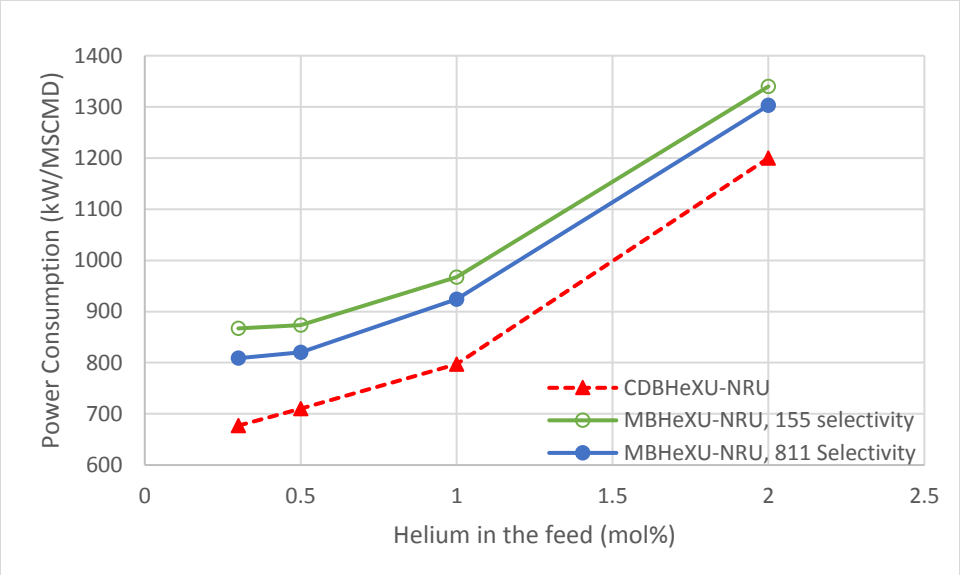

Figure 5. Power consumption comparison for Case A with 15 mol% nitrogen in the NRU feed

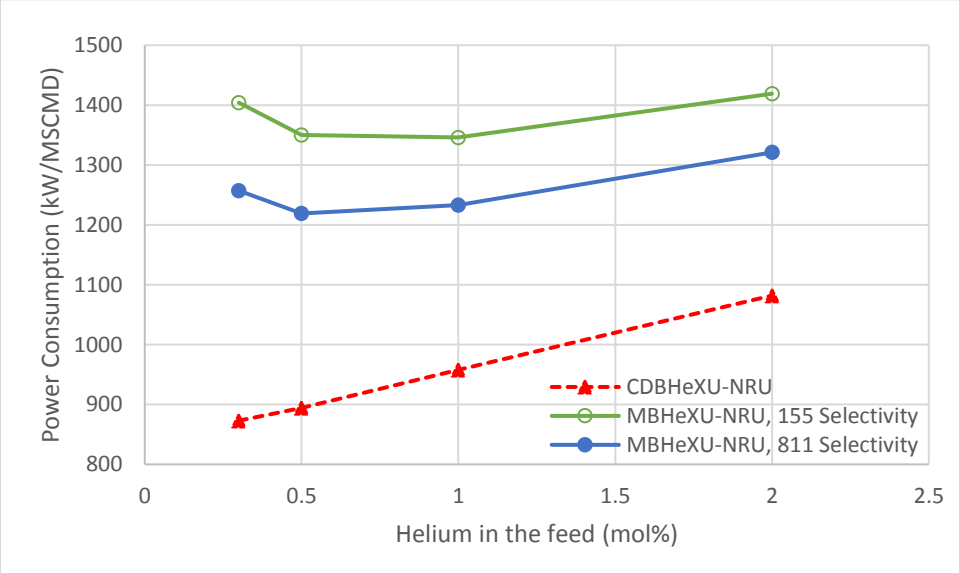

Figure 6. Power consumption comparison for Case A with 30 mol% nitrogen in the NRU feed

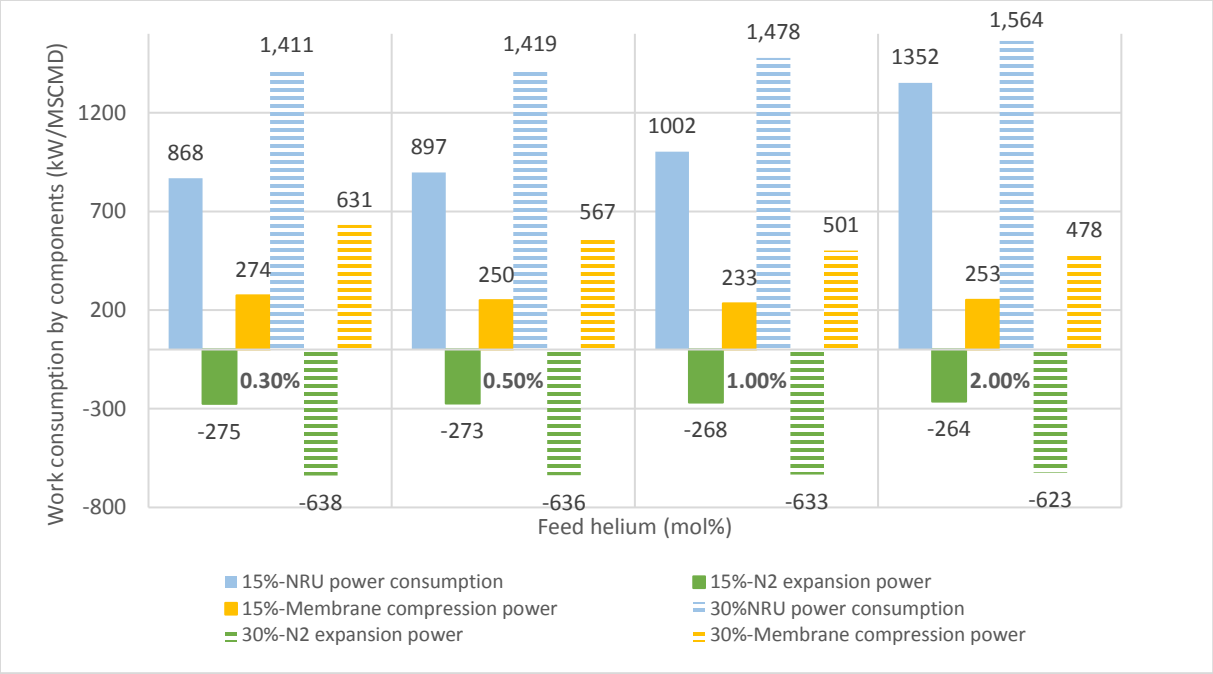

Figure 7. Power consumption distribution for Case A for MBHeXU-NRU with 15 mol% and 30 mol% nitrogen in the feed

5.2 Case B: upgraded helium and atmospheric nitrogen

As shown in Figures 8 and 9, the CD-HeXU-NRU shows a better performance in terms of power consumption for both 15 and 30 mol% nitrogen contents. For the same reason as mentioned earlier, the power consumption differences between the MB-HeXU-NRU and the CD-HeXU-NRU are larger for 30 mol% nitrogen.

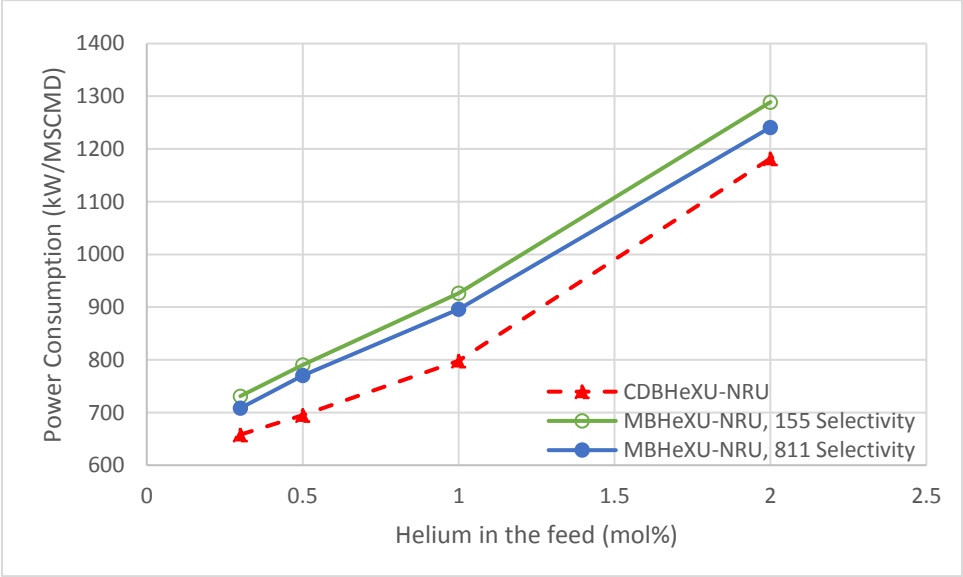

Figure 8. Power consumption comparison for Case B with 15 mol% nitrogen in the NRU feed

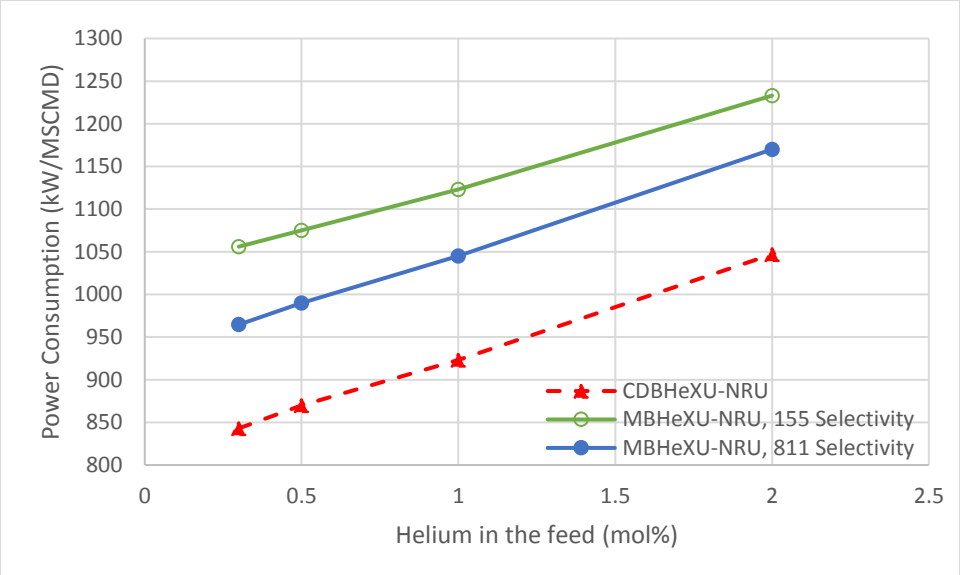

Figure 9. Power consumption comparison for Case B with 30 mol% nitrogen in the NRU feed

5.3 Case C: upgraded helium and pressurized nitrogen

According to Figures 10 and 11, the opposite outcome can be seen in Case C, as opposed to the two previous cases. In Case C, the MBHeXU-NRU has less power consumption for 15 mol% nitrogen over the whole range of helium and 30 mol% nitrogen with helium contents higher than 0.5 mol%. Whether these power reductions are economically beneficial for the project should be discussed further. The discussion is elaborated in the next section. As expected, the MBHeXU-NRU with selectivity 811 has a lower power consumption compared to selectivity 155. As discussed earlier, the membrane with selectivity 811 is not a viable choice and will be excluded in Section 6 as it has very low permeability. The only intention of considering this high value for selectivity is to show that the power requirement differences are not significant even when the highest available selectivity for He/N2 separation is assumed.

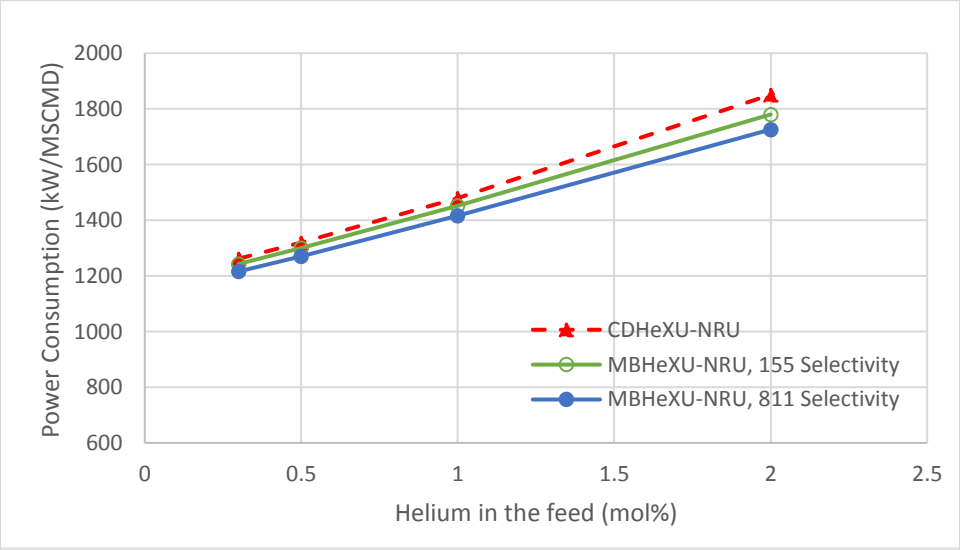

Figure 10. Power consumption comparison for Case B with 15 mol% nitrogen in the NRU feed

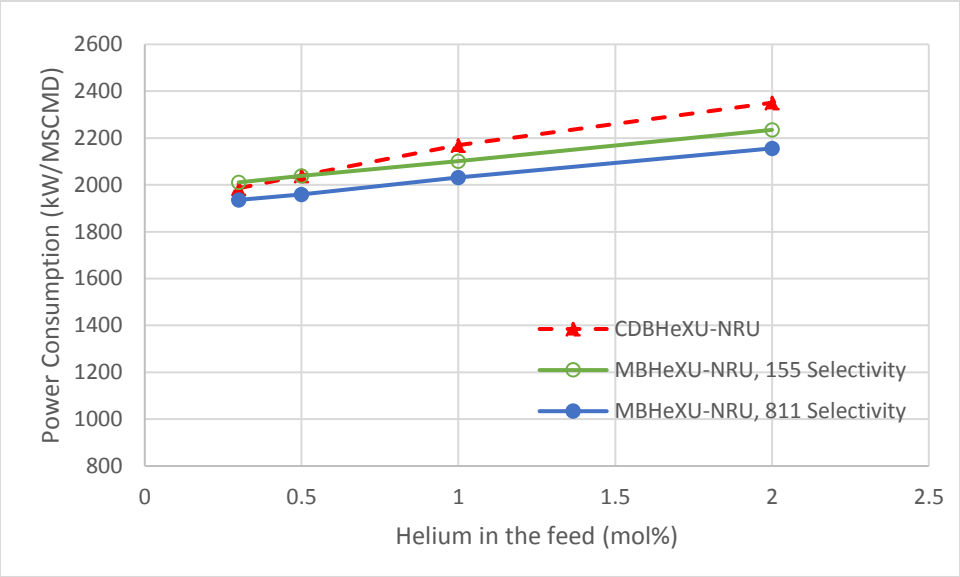

Figure 11. Power consumption comparison for Case B with 30 mol% nitrogen in the NRU feed

6 Economic Analysis

In Sections 5-1 and 5-2, it was shown that the MBHeXU-NRU system consumes more energy compared to the CDBHeXU-NRU for Cases A and B. Although the cost of the two membranes is much less than the total cost of the cryogenic distillation column and the MSHE-201, the extra compressor (K-202), which is required only for the membrane scheme, results in the higher capital cost for the membrane system. In fact, K-202 is considered one of the main costs in the MBHeXU-NRU process because this compressor is a three-stage compressor with pressure ratio 20-25. As a result, this suggests that the CDBHeXU-NRU design is always better than the MBHeXU-NRU system in terms of energy and capital costs.

In contrast, according to Figures 10 and 11, the MBHeXU-NRU system shows better performance in terms of power consumption for Case C except when helium is less than 0.5 mol% for 30 mol% nitrogen. However, for a better comparison of the two processes, an economic analysis is adopted as a final assessment technique. For this purpose, the Net Present Value (NPV) method was used, which is one of the common techniques to evaluate and compare investments. The NPV analysis by itself can be used as a practical and strategic indicator of a project. However, it may alternatively be utilized to eliminate the time effect of the future net cash flows in order to determine other key economic parameters. In our analysis, we used this approach to estimate the break-even price of the electricity in which the operating cost differences between the two systems become equal to the respective capital cost differences. This break-even price is a turning point above which the MBHeXU-NRU is suggested to reduce the operating costs.

The Aspen Hysys Economic Evaluation package was used to evaluate equipment costs and the MSHE costs were estimated using the approach of Hewitt and Pugh, 2007. The membrane module and framework costs are calculated based on Eq.2 (Van Der Sluijs et al., 1992).

$$Membrane\ Capital\ Cost = CC_{mm} + CC_{mf} = A_m C_m + \left(\frac{A_m}{2000}\right)^{0.7} C_{mf} \qquad \text{Eq. (2)}$$

where CC_{mm} and CC_{mf} are the capital cost of the membrane module and its frame respectively. A_m, C_m and C_{mf} are membrane area (m^2), membrane module price per unit ($/m^2) and membrane frame price (M$). C_m and C_{mf} are assumed to be 50 $/m^2 and 0.238 M$ respectively (Van Der Spek et al., 2018, Van Der Sluijs et al., 1992).

Table 3 shows total capital costs for the two processes. Four scenarios with different lifetimes and discount rates are defined. Based on the capital cost and power consumption differences, the break-even electricity prices are presented for each scenario. In other words, for any electricity tariff higher than the break-even values, the membrane system is recommended. In fact, the electricity supply in the industry sector rarely goes beyond 150 $/MWh. This implies that for those cases of which the break-even price is higher than 150 $/MWh, the CDBHeXU-NRU design can always be suggested.

Based on the results of the cases with 30 mol% nitrogen, one may conclude that the MBHeXU-NRU system is dominantly a better option when helium increases in the HeXU feed. Based on this conclusion, we may expect the superiority of the membrane choice for 15 mol% nitrogen cases since the helium concentration is higher in the HeXU feed. However, the results show the opposite. This is because, for 15 mol% nitrogen, a smaller portion of the main feed flows into the HeXU as compared with the 30 mol% nitrogen case. Thus, the power consumption differences for 15 mol% nitrogen decrease proportionally to the HeXU feed flowrate and cannot justify the high capital cost of the membrane system. This also implies that the break-even prices can vary with the main feed flowrate and the portion that flows into the HeXU. Hence, in Case C, the technology selection depends on the feed flowrate and composition, the electricity tariff, and economic parameters of a particular project.

Nevertheless, it can be concluded that the membrane system shows better performance when both nitrogen and helium increase in the main feed provided that the nitrogen product is required at high pressure as it is in Case C.

Table 3. Economic evaluation for Case C with different scenarios for the plant's life time and discount rate

Nitrogen content (mol%)	**15**				**30**			
Helium content (mol%)	0.3	0.5	1	2	0.3	0.5	1	2
Total capital cost-membrane-based, MUSD	12.16	12.25	12.55	13.61	13.04	13.07	13.11	13.38
Total capital cost-cryogenic distillation, MUSD	11.61	11.70	11.88	12.25	12.20	12.30	12.45	12.69
Capital cost difference, MUSD	0.55	0.55	0.67	1.36	0.84	0.77	0.66	0.69
Power consumption difference, kW	19	20	28	71	-25	~0	69	116
Different scenarios	**Break-even electricity price, $/MWh**							
Scenario 1: 15 years lifetime & 5% discount rate	264.4	251.4	218	176.21	---	---	88.7	54.5
Scenario 2: 15 years lifetime & 10% discount rate	360.8	343.2	298.7	240	---	---	121.0	74.3
Scenario 3: 7 years lifetime & 5% discount rate	474.2	451.1	392.6	316.1	---	---	159.1	97.7
Scenario 4: 7 years lifetime & 10% discount rate	563.6	536.1	466.7	357.7	---	---	189.1	116.1

7 Conclusion

This study proposed an integrated scheme for membrane-based and cryogenic distillation-based helium separation systems with a single-column NRU and evaluated and compared them for different applications. Matlab programming was used to model the membrane system and incorporate it into Aspen Hysys, which is used to simulate the rest of the process flowsheet. Next, the entire system was optimized using the particle swarm optimization method. The results show that when the nitrogen is considered effluent and released

into the atmosphere, the cryogenic distillation technology outperforms the membrane system due to the significant advantages in both power consumption and capital costs. The cryogenic process can reduce the power consumption by 10-40%. In contrast, when the nitrogen product is needed at high pressure and the helium concentration is not very small in the HeXU feed, the MBHeXU consumes less energy compared with the CDBHeXU (maximum 5% reduction). However, it still accounts for higher capital costs compared to cryogenic distillation separation due to a more expensive compression system. Thus, the final decision of the technology selection depends on feed flowrate, feed condition, local energy cost, plant lifetime and the discount rate of a project.

8 Appendix A

The material balance of helium for the second-stage membrane (Mem-202) can be written as follows:

$$F_{SN-206}x_{He,SN-206} = F_{SN-209}x_{He,SN-209} + F_{SN-208}x_{He,SN-208} \quad \text{Eq. (A.1)}$$

$$F_{SN-206}x_{He,SN-206} = F_{SN-204}x_{He,SN-204} \quad \text{Eq. (A.2)}$$

where F and x_{He} are molar flowrate and helium mole fraction of the corresponding stream respectively. Thus we can rewrite the Eq.A-1:

$$F_{SN-208}x_{He,SN-208} = F_{SN-204}x_{He,SN-204} - F_{SN-209}x_{He,SN-209} \quad \text{Eq. (A.3)}$$

RecoveryMem-201 is defined as follows:

$$Recovery_{Mem-201} = \frac{F_{SN-204}x_{He,SN-204}}{F_{SN-202}x_{He,SN-202}+F_{SN-208}x_{He,SN-208}} \quad \text{Eq. (A.4)}$$

The combination of the Eqs.A-3 and A-4 yields:

$$Recovery_{Mem-201} = \frac{F_{SN-204}x_{He,SN-204}}{F_{SN-202}x_{He,SN-202}+F_{SN-204}x_{He,SN-204}-F_{SN-209}x_{He,SN-209}} \quad \text{Eq. (A.5)}$$

Eq.A-5 can be rewritten:

$$\frac{1}{Recovery_{Mem-201}} = 1 - \frac{F_{SN-209}x_{He,SN-209}}{F_{SN-204}x_{He,SN-204}} + \frac{F_{SN-202}x_{He,SN-202}}{F_{SN-209}x_{He,SN-209}} \times \frac{F_{SN-209}x_{He,SN-209}}{F_{SN-204}x_{He,SN-204}} \quad \text{Eq. (A.6)}$$

Given that RecoveryMem-202 and Recoverytotal are defined:

$$Recovery_{Mem-202} = \frac{F_{SN-209}x_{He,SN-209}}{F_{SN-206}x_{He,SN-206}} = \frac{F_{SN-209}x_{He,SN-209}}{F_{SN-204}x_{He,SN-204}} \quad \text{Eq. (A.7)}$$

$$Recovery_{total} = \frac{F_{SN-209}x_{He,SN-209}}{F_{SN-202}x_{He,SN-202}} \quad \text{Eq. (A.8)}$$

The following equation can be established by substituting Eqs.A-7 and A-8 into Eq.A-6:

$$Recovery_{Mem-202} = \frac{1-{}^{1}/_{Recovery_{Mem-201}}}{1-1/Recovery_{total}} \quad \text{Eq. (A.9)}$$

9 Acknowledgements

Homa Hamedimastanabad acknowledges the financial support under the SINGA scholarship. The work was also funded in part by the National University of Singapore through a seed grant (R261–508 -001–646/733) for CENGas (Center of Excellence for Natural Gas).

10 Nomenclature

CDBHeXU= cryogenic distillation-based HeXU

Con= condenser in Figures 3 and 4

CW= cooling water heat exchanger in Figures 3 and 4

E= expander in Figures 3 and 4

EGR= enhanced gas recovery

EOR= enhanced oil recovery

F= flowrate in Table 1

HeXU= helium extraction unit

K= compressor in Figures 3 and 4

LNG= liquefied natural gas

MBHeXU= membrane-based HeXU

Mem= membrane station in Figures 3 and 4

Min= minimum

MSHE= multi-stream heat exchanger

NG= natural gas

NPV= net present value

NRU= nitrogen rejection unit

PFD= process flow diagram

PNG= pipeline natural gas

Press= pressure in Table 1

PSA= pressure swing adsorption

Reb= reboiler in Figures 3 and 4

SHR= self-heating reboiler

SN= stream number in Figures 3 and 4

SR= split Ratio in Table 1

T= distillation column in Figures 3 and 4

Tem= temperature in Table 1

V= separator in Figures 3 and 4

VF= vapor Fraction in Table 1

VL= valve in Figures 3 and 4

11 References

Alders, M., Winterhalder, D., Wessling, M., 2017. Helium recovery using membrane processes. *Separation and Purification Technology, 189*, 433-440. doi:10.1016/j.seppur.2017.07.084

Baker, R. W., Wiley, I., 2012. *Membrane technology and applications* (3rd ed.). Oxford: Wiley-Blackwell.

Burite, J. (2016). Scientists Discover 'Game-Changer' Helium Deposits in Tanzania. *Bloomberg*.

Cao, Y., Flores-Cerrillo, J., Swartz, C. L. E., 2017. Practical optimization for cost reduction of a liquefier in an industrial air separation plant. *Computers and Chemical Engineering, 99*, 13-20. doi:10.1016/j.compchemeng.2016.12.011

Clarke, J., McLay, L., McLeskey Jr, J. T., 2014. Comparison of genetic algorithm to particle swarm for constrained simulation-based optimization of a geothermal power plant. *Advanced Engineering Informatics, 28*(1), 81-90. doi:10.1016/j.aei.2013.12.003

Coker, D. T., Freeman, B. D., Fleming, G. K., 1998. Modeling multicomponent gas separation using hollow-fiber membrane contactors. *AIChE Journal, 44*(6), 1289-1300.

Eghbal, M., Saha, T. K., Hasan, K. N., 2011. *Transmission expansion planning by meta-heuristic techniques: A comparison of Shuffled Frog Leaping Algorithm, PSO and GA.* Paper presented at the IEEE Power and Energy Society General Meeting.

Elbeltagi, E., Hegazy, T., Grierson, D., 2005. Comparison among five evolutionary-based optimization algorithms. *Advanced Engineering Informatics, 19*(1), 43-53. doi:10.1016/j.aei.2005.01.004

Gottschlich, D. E., Roberts, D. L., Wijmans, J. G., Bell, C. M., Baker, R. W., 1989. Economic comparison of several membrane configurations for H2/N2 separation. *Gas Separation and Purification, 3*(4), 170-179. doi:10.1016/0950-4214(89)80002-7

Hamedi, H., Karimi, I. A., Gundersen, T., 2018. Optimal cryogenic processes for nitrogen rejection from natural gas. *Computers and Chemical Engineering, 112*, 101-111. doi:10.1016/j.compchemeng.2018.02.006

Hassan, R., Cohanim, B., De Weck, O., Venter, G., 2005. *A comparison of particle swarm optimization and the genetic algorithm.* Paper presented at the Collection of Technical Papers - AIAA/ASME/ASCE/AHS/ASC Structures, Structural Dynamics and Materials Conference.

Hewitt, G. F., Pugh, S. J., 2007. Approximate design and costing methods for heat exchangers. *Heat Transfer Engineering, 28*(2), 76-86. doi:10.1080/01457630601023229

Kennedy, J., Eberhart, R., 1995. *Particle swarm optimization.* Paper presented at the IEEE International Conference on Neural Networks - Conference Proceedings.

Kim, D., Gundersen, T., 2015. Helium extraction from LNG end-flash. *Chemical Engineering Transactions, 45*, 595-600. doi:10.3303/CET1545100

MacKenzie, D., Cheta, I., Burns, D., 2002. Removing nitrogen. *Hydrocarbon Engineering, 7*(11), 57-63.

Merkel, T. C., Lin, H., Wei, X., Baker, R., 2010. Power plant post-combustion carbon dioxide capture: An opportunity for membranes. *Journal of Membrane Science, 359*(1-2), 126-139. doi:10.1016/j.memsci.2009.10.041

Panduro, M. A., Brizuela, C. A., Balderas, L. I., Acosta, D. A., 2009. A comparison of genetic algorithms, particle swarm optimization and the differential evolution method for the design of scannable circular antenna arrays. *Progress In Electromagnetics Research B*(13), 171-186. doi:10.2528/PIERB09011308

Rufford, T. E., Smart, S., Watson, G. C. Y., Graham, B. F., Boxall, J., Diniz da Costa, J. C., May, E. F., 2012. The removal of CO2 and N2 from natural gas: A review of conventional and emerging process technologies. *Journal of Petroleum Science and Engineering, 94-95*, 123-154. doi:10.1016/j.petrol.2012.06.016

Sadeghzadeh, H., Ehyaei, M. A., Rosen, M. A., 2015. Techno-economic optimization of a shell and tube heat exchanger by genetic and particle swarm algorithms. *Energy Conversion and Management, 93*, 84-91. doi:10.1016/j.enconman.2015.01.007

Scholes, C. A., Ghosh, U., 2016. Helium separation through polymeric membranes: selectivity targets. *Journal of Membrane Science, 520*, 221-230. doi:10.1016/j.memsci.2016.07.064

Scholes, C. A., Gosh, U. K., Ho, M. T., 2017. The Economics of Helium Separation and Purification by Gas Separation Membranes. *Industrial and Engineering Chemistry Research, 56*(17), 5014-5020. doi:10.1021/acs.iecr.7b00976

Siddhartha, Sharma, N., Varun, 2012. A particle swarm optimization algorithm for optimization of thermal performance of a smooth flat plate solar air heater. *Energy, 38*(1), 406-413. doi:10.1016/j.energy.2011.11.026

Soleimany, A., Hosseini, S. S., Gallucci, F., 2017. Recent progress in developments of membrane materials and modification techniques for high performance helium separation and recovery: A review. *Chemical Engineering and Processing: Process Intensification, 122*, 296-318. doi:10.1016/j.cep.2017.06.001

Van Der Sluijs, J. P., Hendriks, C. A., Blok, K., 1992. Feasibility of polymer membranes for carbon dioxide recovery from flue gases. *Energy Conversion and Management, 33*(5), 429-436. doi:https://doi.org/10.1016/0196-8904(92)90040-4

Van Der Spek, M., Bonalumi, D., Manzolini, G., Ramirez, A., Faaij, A., 2018. Techno-economic Comparison of Combined Cycle Gas Turbines with Advanced Membrane Configuration and Monoethanolamine Solvent at Part Load Conditions. Energy&Fuels, 32, 625−645. doi:https://doi.org/ 10.1021/acs.energyfuels.7b02074